Journal of Biomechanics 168 (2024) 112097

Contents lists available at ScienceDirect

Journal of Biomechanics

journal homepage: www.elsevier.com/locate/jbiomech

Intersegmental coordination in human slip perturbation responses

Vaibhavsingh Varma, Mitja Trkov *

Mechanical Engineering, Henry M. Rowan College of Engineering, Rowan University, Glassboro, NJ 08028, USA

ARTICLE INFO

Keywords:
Human locomotion
Slip recovery
Intersegmental coordination
Planar covariation law
Limb elevation angles

ABSTRACT

Intersegmental coordination (ISC) of lower limbs and planar covariation law (PCL) are important phenomena observed in biomechanics of human walking and other activities. Gait perturbations tend to cause deviation from the expected ISC pattern thus violating PCL. We used a data set of seven subjects, who experienced unexpected slips, to investigate and characterize the evolution of ISC during slip recoveries and falls. We have analyzed and presented the development of ISC patterns, encompassing the step preceding the slip initiation and duration of slip until it stops. The results show that the ISC patterns during slip recovery deviate considerably from the normal walking patterns. A newly proposed Euclidian distance-based metric (EDM) was used to quantify the deviation from the normal walking ISC pattern during four slip recoveries and three falls evaluated at gait events such as slip start, foot strike, and peak height of the swing foot. The timing of gait events after slip, pattern of EDM, placement of the feet after slip and temporal patterns of each limb angle have been presented. This initial investigation provides insight into the ISC during slip recovery which highlights the human natural recovery trajectories during such perturbations. The observed patterns of the ISC trajectories during slip can be used for the design of human-inspired controllers for exoskeleton devices that can provide external assistance to human subjects during balance recovery.

1. Introduction

Stable human locomotion requires precise intersegmental limb coordination. The elevation angles of the lower limb segments i.e., thigh, shank, and foot, covary along a plane during walking (Borghese et al., 1996) which is defined as the planar covariation law (PCL). Previous studies have observed planar covariations during normal walking (Bianchi et al., 1998; Borghese et al., 1996), walking on inclined surfaces (Ivanenko et al., 2008; Noble and Prentice, 2008) staircase stepping (Ivanenko et al., 2008), and crouched or bent walking (Grasso et al., 2000; Ivanenko et al., 2008). The planar covariation of the lower limb elevation angles was shown to develop among toddlers learning to walk (Cheron et al., 2001; Ivanenko et al., 2005). Patients having rheumatoid arthritis with forefoot impairment adapt to planar covariation, however, with different elevation angle patterns (Laroche et al., 2006). In addition, patients with a hereditary spastic paraparesis also show planar covariation of limb elevation angles, although with abnormal orientation and shape (Dan et al., 2000). These studies suggest the importance of investigating the intersegmental coordination (ISC) and PCL that can provide insights in better understanding the human motor control and coordination during locomotion. The locomotion patterns and ISC during perturbations are also crucial during recovery response to prevent falls. Among the existing studies investigating ISC and PCL during gait perturbations, Aprigliano et al. (2019) reported that PCL is violated after a slip perturbation. Further investigations of utilizing ISC and PCL beyond walking can broaden our knowledge of ISC during gait perturbations.

The kinematic parameters such as slipping heel velocity and slipping distance are determining factors for slip severity (Lockhart et al., 2002; Redfern et al., 2001). Additionally, the biomechanical parameters at trailing leg touch down are important in slip recovery (Rasmussen and Hunt, 2021). In addition, Nazifi et al. (2020) observed that the magnitude of body angular momentum indicates severity of slip, while ageing degrades the ability to recover from slips because the recovery response becomes slower and less effective (Lockhart et al., 2005). However, none of these parameters have been investigated in relation to the ISC during slip. Observing the effect of spatiotemporally asymmetric gait on coordination and whole-body angular momentum, (Liu and Finley, 2020) have emphasized the need for exploration of changes in intersegmental coordination patterns. Furthermore, a need for better fall prevention

* Corresponding author at: Department of Mechanical Engineering, Henry M. Rowan College of Engineering, Rowan University, 201 Mullica Hill Rd., Glassboro, NJ 08028, USA.
E-mail address: trkov@rowan.edu (M. Trkov).

https://doi.org/10.1016/j.jbiomech.2024.112097
Accepted 14 April 2024
Available online 16 April 2024

strategies was emphasized by Chang et al. (2016). Investigating ISC and PCL during slip gaits in relation to the established slip kinematic parameters can provide better understanding of slip severity and human balance recovery responses and enable creation of new fall prevention strategies.

The purpose of this study was to investigate and characterize the behavior of the kinematic-based ISC manifolds for gaits after slip occurrence. We hypothesized that the differences between the ISC manifolds during walking and after slip onset can be characterized and compared at the specific gait events to reflect the differences in patterns between slip recoveries and falls. Our specific objective was to characterize these differences using Euclidian distance-based metric (EDM) and use it to explain the differences in kinematic behavior between recoveries and falls.

2. Methods

We used and analyzed de-identified data from slip detection study in (Trkov et al., 2019). It contains data from unexpected slip experiments for eight subjects. It includes measurements of the optical markers from motion capture system and the inertial measurements units. Markers and IMUs were attached to the trunk and lower limbs (i.e., thigh, shank, and foot) and the sampling frequency of the kinematic data was 100 Hz. In our study, only motion capture data was used and one (male) subject was omitted due to missing a small portion of data required in our analysis. The analyzed data contains trials representing four subjects who recovered after slip and three subjects who fell. This initial investigation, which involves a small group of participants, was purposefully chosen as it includes both the recovery and falling experiences of these individuals. Furthermore, the data contains a single and multi-step recovery, which is challenging to obtain due to the unpredictable responses of each participant. In this context, the data contains one instance of a double slip where the participant successfully recovered and another double slip instance resulting in a fall, while the remaining participants encountered single-leg slips. The data was processed in MATLAB 2022b (MathWorks, Inc., Natick, MA) using a custom script.

Elevation angles in the sagittal plane were computed as Euler angles between the vertical and the 3D unit vectors along the line segments joining hip and knee markers for thigh angle (θ_t), knee and ankle markers for shank angle (θ_s), and heel and toe markers for the foot elevation angle (θ_f), as shown in Fig. 1. The elevation angles were then normalized by subtracting the mean value in accordance with previous studies (Aprigliano et al., 2019; Borghese et al., 1996; Ivanenko et al., 2008). Normalization centers the ISC manifold about the origin of the coordinate system where the angles θ_t, θ_s, and θ_f, form the axes. The normalization enables the inter-subject comparison.

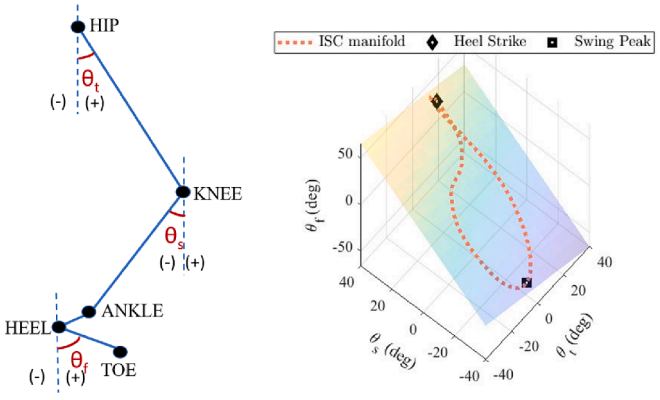

Fig. 1. (A) Representation of the markers, elevation angles and sign convention. θ_t, θ_s, and θ_f respectively represent thigh, shank, and foot elevation angles. (B) ISC manifold and corresponding PCL plane for one representative normal walking gait cycle showing the Heel Strike and Swing Peak events.

Fig. 1 shows the representative ISC manifold with marked gait events and counterclockwise progression. Gait events were identified using a combination of the foot elevation angles and vertical heel marker (HM) position. Heel strike for normal walking occurs at the first minimum of HM immediately after the foot angle reaches its maximum positive value in one gait cycle. For reference purposes, we considered the peak height of the swing foot (referred to as *swing peak*). This event occurs shortly after the toe-off, and it is more consistent and easier to identify compared to toe-off, which may not always be present during slip recovery. The *swing peak* event was determined as the highest vertical position of the HM during the swing phase when the foot angle is at its minimum. During slip recovery, we identified the *foot strike* event as the instance when the heel makes contact with the floor. It is important to note that this differs from a natural heel strike where the first point of contact is always the heel, which may not always be the case in perturbed gait. We relied solely on the HM position to mark it, identifying it whenever the HM reached its lowest position during the gait cycle at multiple instances particularly during multi-step recovery process.

An Euclidian distance-based metric (EDM) has been introduced to quantify the deviation of the ISC manifold from the expected normal walking manifold (represented by the blue curve in Figs. 2 and 3) during slip perturbation. EDM was computed as the Euclidian distance between the normal and slip ISC manifolds at foot strike and swing peak events. Foot strikes after slip are compared with the heel strike on the normal walking manifold. Swing peak event is used as a reference for comparison because it represents an extreme position on the ISC manifold that is easy to identify even after slip onset. We computed EDM at the heel strike and swing peak events for level walking trials of several subjects of different ages (19 – 67 years), walking at different speeds (0.18–2.3 m.s-1) taken from a large gait data set. This data set, that includes fifty subjects, has been made openly available by Schreiber & Moissenet (2019). The EDM was computed between two gait cycles of each subject. The results were then averaged and the standard deviation of the calculated EDM at each event were computed. These values have been used as a reference for comparing the slip gait EDM. In addition, foot placement at the first and second foot strikes after slip were computed in terms of distance from the projection of center of mass (COM) on the ground. The COM was computed using a body segment approach (Nazifi et al., 2020) and the segments' masses and COMs were considered as per empirical relations in (Winter, 2009). Several other variables were used in conjunction with the EDM, foot placement, and the temporal profiles of individual limb elevation angles to distinguish between slip recoveries and falls. Slipping heel velocities and slipped distance up to the maximum slipping heel velocity were estimated using the horizontal HM position along the walking/antero-posterior direction. Hip height variation was considered as the vertical distance of the midpoint between the two hip markers (Pai and Bhatt, 2007).

3. Results

ISC manifolds for the trailing and slipping legs of individual subjects are represented in Figs. 2 and 3, respectively. In both figures, parts A-D represent recoveries, while parts E-G represent falls. Analysis of the ISC manifolds shows that the trailing leg progresses similar as during normal walking until the *swing peak 1* event (occurs 160 ms to 230 ms after slip onset); see Table 1. Afterwards, the human voluntary recovery reaction starts and the slip ISC manifolds start to deviate from the normal walking manifold. This is also evident from Fig. 4A which shows the EDM for trailing leg at significant gait events after slip. The EDM does not change much for the recovered subjects from *slip start* to *swing peak 1* for the trailing leg with the average value of 7.5 deg, which is within the standard deviation range (5.8 ± 3.6 deg) of normal walking EDM at this event. Figs. 3 and 4B show increased EDM and suggest that the PCL is violated for the slipping leg before the *swing peak 1* event, which is valid because the leg is slipping and following normal gait.

Fig. 2E-G and 3E-G show deviation of the trailing leg ISC curves from

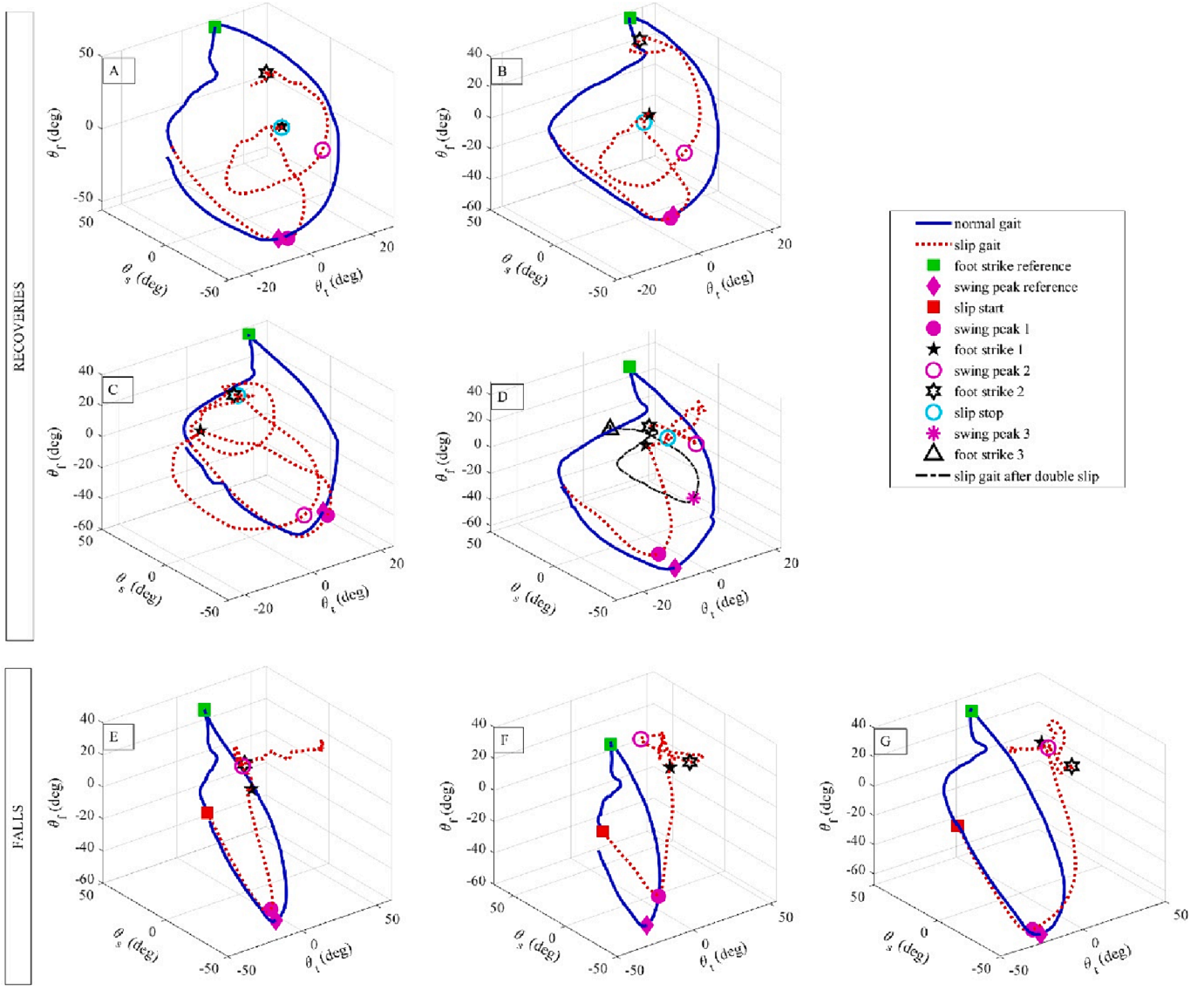

Fig. 2. ISC manifolds for the trailing leg for subjects (A) Sub1, (B) Sub2, (C) Sub3, (D) Sub4, (E) Sub5, (F) Sub6, and (G) Sub7.

the PCL plane for the subjects who experienced a fall. Those trajectories never return to the PCL plane as compared to those who recovered from slip. All subjects except Sub4 and Sub5 stepped with their trailing leg on the non-slippery surface. The peak EDM values and EDM profiles for the subjects who experienced a fall in Fig. 4A and 4B are on average higher compared to those that recovered (see Table 1). Importantly, the proposed EDM metric for the slipping leg shows increase in deviation from the normal walking profile for all fallers and importantly distinguishes falls from recoveries (Fig. 4B). This deviation is clear during *foot strike 1* for the single leg slip (Sub6 and Sub7) or during *foot strike 2* for the double leg slip (Sub5).

Figs. 4C-D show the foot placement of all subjects at the *foot strike 1* and *foot strike 2* events, respectively. The trailing foot for all recovered subjects remains behind the projected COM, while two of the subjects who experienced a fall (Sub6 and Sub7) placed their trailing foot ahead of the projected COM. Although, one subject who experienced a fall (Sub5) managed to place the trailing foot behind the projected COM, it was placed on a slippery surface causing trailing foot to slip and become unstable. Therefore, the slipping foot could not become stationary, which can be observed from the heel velocity profile of the slipping and trailing legs in Fig. 5E. One recovered subject (Sub4) also suffered a similar double slip, with a similar trailing foot placement as Sub5 (see Fig. 4C). However, as shown in Fig. 5D, their slipping foot was able to become stationary (by hitting the non-slippery surface), thus providing momentary stability. Furthermore, it is important to note, that the Sub4 had the shortest time (260 ms) from slip onset to *foot strike 1*, which is an important factor contributing to successful recovery even after double slip. All other recovered subjects were able to momentarily make their trailing foot stationary after *foot strike 1* as shown in Fig. 5A-C. The hip height for all the recovered subjects ended above the mean hip height of normal gait before *foot strike 2*, whereas the hip height did not increase for subject Sub6 and Sub7 (see Fig. 5F and 5G). Although, subject Sub5 could potentially regain hip height, the constant slipping of both feet in the forward direction prevented recovery and hip height lowered back again before *foot strike 2* (Fig. 5E).

The temporal behaviors of the thigh, shank, and foot elevation angles, presented as non-normalized absolute values as opposed to those of the ISC manifolds, are shown in Figs. 6, 7, and 8, respectively. For recoveries, the thigh angles vary in a manner similar to that of normal gait until *swing peak 1*, and tend to converge to a similar value at that instant with a magnitude of 23.4 ± 1.3 deg. This result signifies that both thighs align momentarily as the trailing leg is in compensatory swing phase (except for Sub4 in Fig. 6D, which exhibits slip of trailing leg). Subsequently, the limbs diverge with the trailing thigh going backward as the

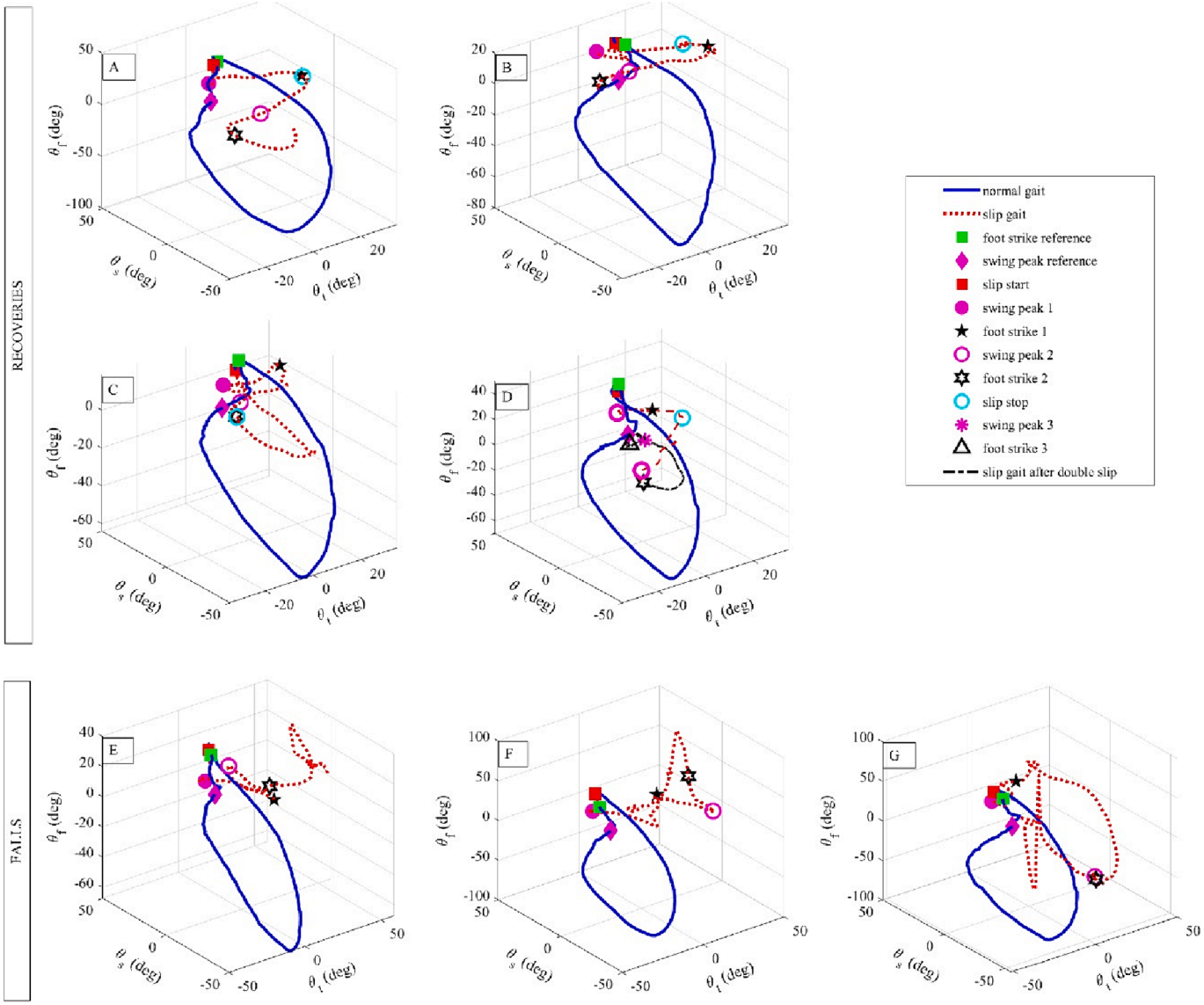

Fig. 3. ISC manifolds for the slipping leg for subjects (A) Sub1, (B) Sub2, (C) Sub3, (D) Sub4, (E) Sub5, (F) Sub6, and (G) Sub7.

Table 1
Slip related metrics for all subjects.

Subject	Walking Speed (m/s)	Max Slip Speed (m/s)	Slip Distance * (m)	Gait Event Timing after slip start (ms)				Maximum EDM	
				Swing Peak 1	Foot Strike 1	Swing Peak 2	Foot Strike 2	Slipping Leg	Trailing Leg
1 (Rec.)	1.3865	2.1755	0.292	190	400	870	1050	68.5	72.7
2 (Rec.)	1.0917	2.254	0.165	190	390	840	1110	73.1	67.9
3 (Rec.)	1.0185	2.3544	0.375	220	410	750	940	59.6	59.9
4 (Rec.)	1.2635	1.9944	0.313	160	260	830	920	63.4	72.4
5 (Fall)	0.9468	1.6042	0.179	230	360	640	740	60.8	84.9
6 (Fall)	1.3395	2.9464	0.401	190	410	680	900	109.3	142.2
7 (Fall)	1.4394	2.9811	0.463	160	350	990	1060	90.5	108.6
	Mean (Rec.)	2.19 ± 0.15	0.29 ± 0.08	190 ± 24	365 ± 70	822 ± 51	1005 ± 90	66.1 ± 5.8	68.2 ± 5.9
	Mean (Falls)	2.51 ± 0.78	0.35 ± 0.15	193 ± 35	373 ± 32	770 ± 191	900 ± 160	86.9 ± 24.4	111.9 ± 28.8
	Normal Walk	–	–	–	–	–	–	5.8 ± 3.6	5.8 ± 3.6

* Slip distance is considered along walking direction from start of slip to the point when max slip speed is reached.

slipping leg is still sliding forward until *foot strike 1* occurs. For falls, the thigh of a trailing leg continues to move in the forward direction.

Shank angle profiles for the trailing leg proceed in a similar manner as normal walking profile until *swing peak 1* for all subjects (see Fig. 7). After *foot strike 1*, the profile abruptly changes and the rate of change of trailing leg shank angles reduce momentarily to stabilize the leg before approaching peak again. For falls, the negative peak of shank or foot angle after *swing peak 1* is not observed. The foot angle profiles (see Fig. 8) for both legs tend to remain converged after *foot strike 1* indicating the lack of action taken by the trailing leg.

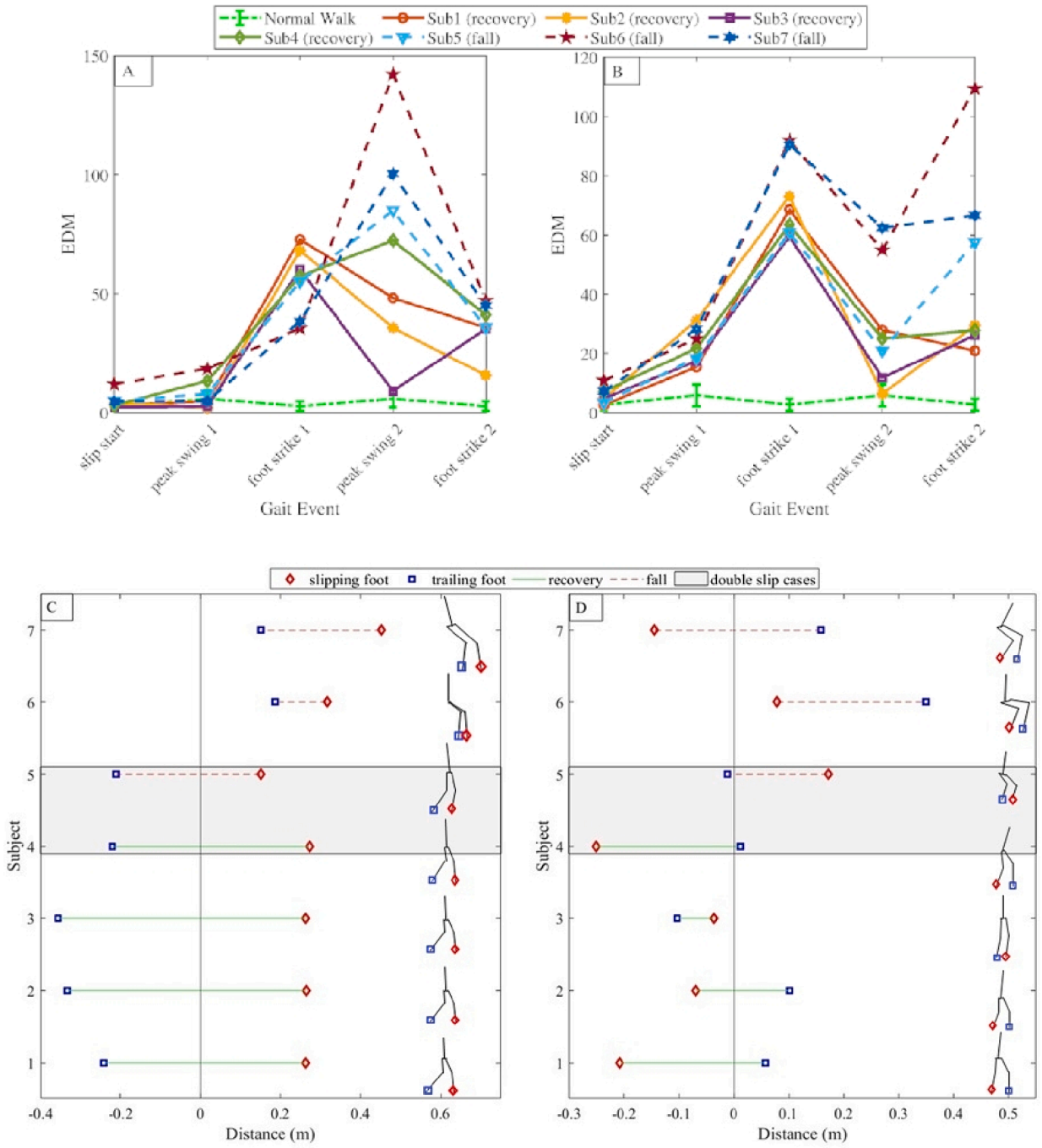

Fig. 4. EDM during slip representing deviations from the expected normal walking ISC manifold for (A) trailing and (B) slipping leg. The normal walking curve represents the mean of EDM computed for two normal walking ISC manifolds across all subjects along with ± 1 standard deviation error bars at each event. Event *slip start* does not exist for normal walking, hence the values considered here correspond to the normal heel strike. Placement of slipping and trailing foot at (C) *foot strike 1* and (D) *foot strike 2* events in terms of distance from the projected COM. Negative value indicates that the foot is behind the projected COM. The stick figures represent bodyconfigurations of each subject at that instant.

4. Discussion

Violation of PCL during gait perturbations has been reported in earlier studies (Aprigliano et al., 2019; Krasovsky et al., 2014; Liu and Finley, 2020). The inspection of ISC during slip recoveries at distinct gait events (i.e., *swing peak* and *foot strike*) of the trailing leg revealed that gait events tend to exhibit similar timings, deviations from the walking ISC manifold (EDM), and temporal patterns of each limb angle during recovery among different individuals. This finding suggests that a general recovery process exists that can be used to develop a control strategy for assistive devices to help prevent slip-induced falls. The results also showed the difference in ISC and recovery patterns for subjects (Sub4 and Sub5) that suffered slip also on trailing leg. Despite both subjects experiencing slip on both legs and Sub5 having the lowest slipping speed (see Table 1), Sub4 was able to recover. Sub5 could not arrest the motion of either foot to regain stability and fell. Successful recovery of Sub4 can be attributed to the shortest reaction times indicated by the shortest timings among all subjects to *swing peak 1* and, most importantly, *foot strike 1*.

Shank and foot elevation angles have been shown to have high

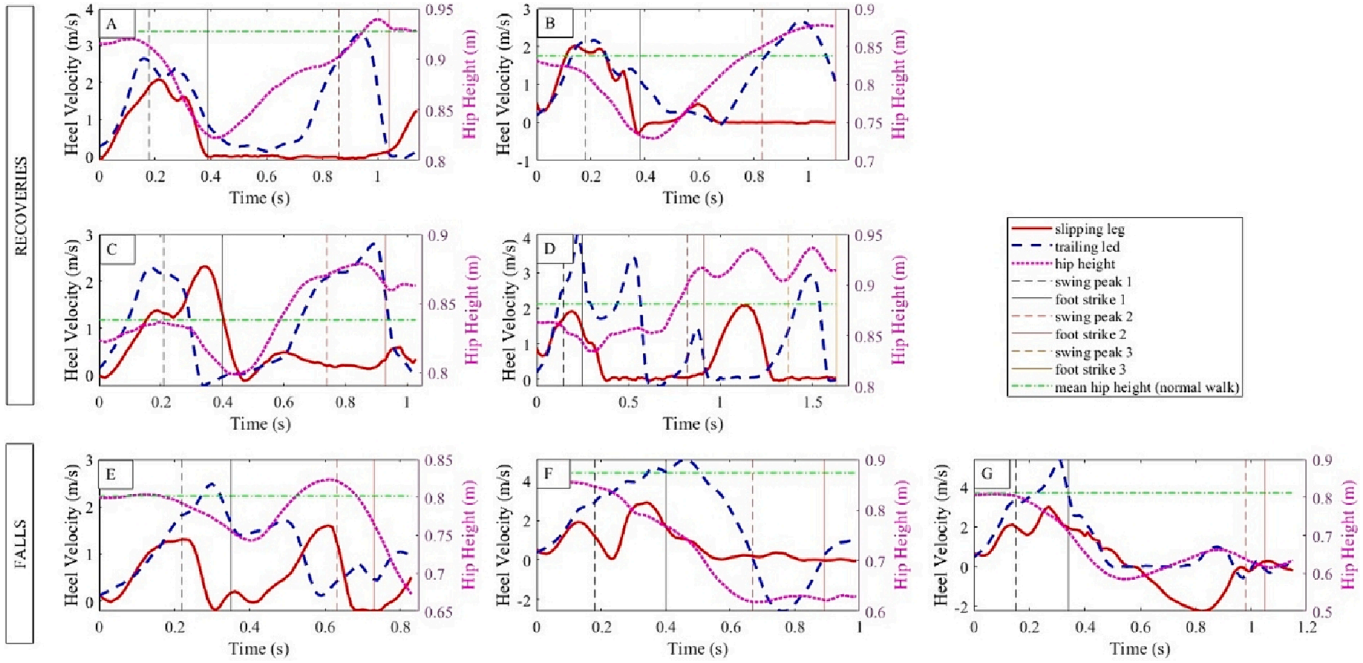

Fig. 5. Heel velocities and hip heights after slip starts for (A-D) recovered subjects (Sub1- Sub4) and (E-F) subjects that experienced a fall (Sub5-Sub7).

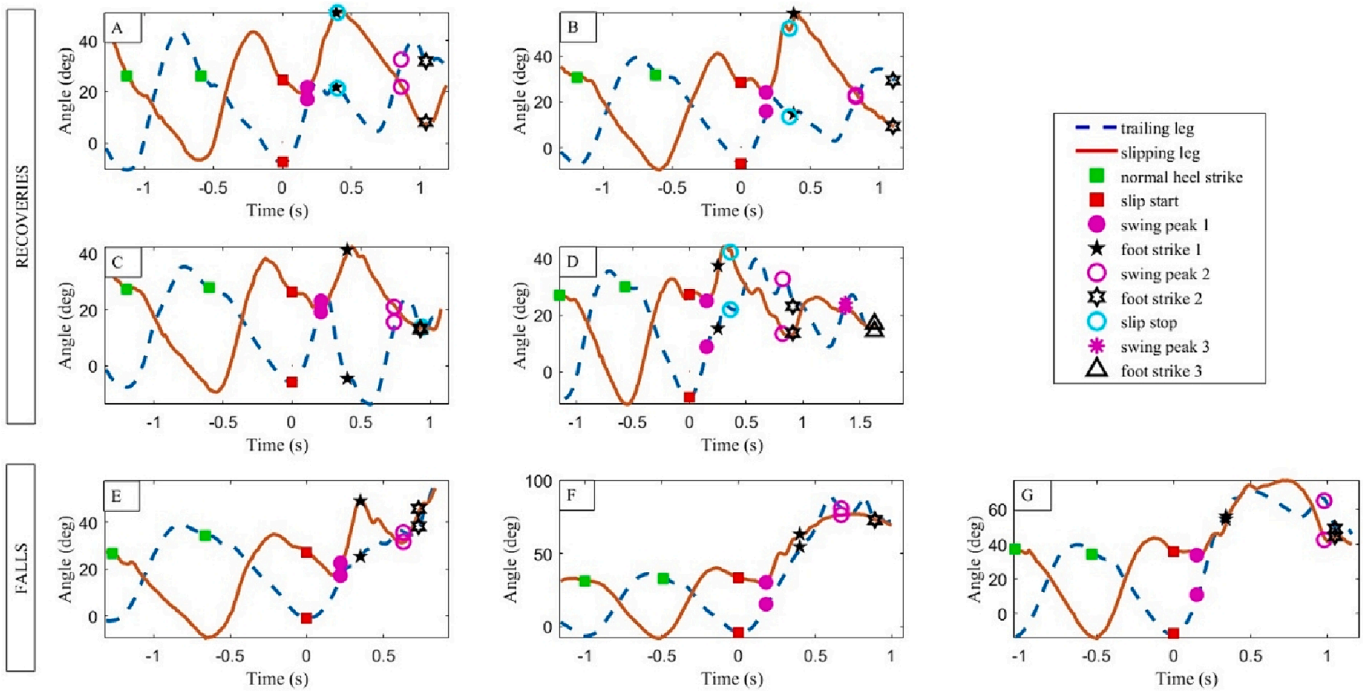

Fig. 6. Thigh angle variations during one complete normal walking gait cycle before and after slip onset. Results for subjects that (A-D) recovered from slip Sub1-Sub4, respectively, and (E-G) subjects that experienced a fall Sub5-Sub7, respectively.

correlation temporally during normal walking (Hicheur et al., 2006). The results of shank and foot profiles in this study indicate their correlation also during slip gaits as observed in Figs. 7 and 8; however, these correlations were not quantitatively assessed in this study.

Overall, parameters such as foot placement location, EDM, and high slip velocity were able to clearly differentiate between recoveries and falls during first foot strike during single leg slip or second foot strike during double leg slip. Future studies may further investigate and analyze slip perturbations with multiple consecutive steps on a slippery surface after slip onset that were not included in this study.

Similar analyses of limb ISC can be conducted to assess the changes in ISC patterns during recovery from trips as well. Importantly, these metrics and observations, especially the slip ISC patterns and timings of distinct kinematic events during recovery, can be used in future studies to develop human-inspired control algorithms for exoskeleton devices to assist during recovery. The exact nature of ISC after perturbations required for successful recovery could be modelled and tested using assistive devices to help prevent falls.

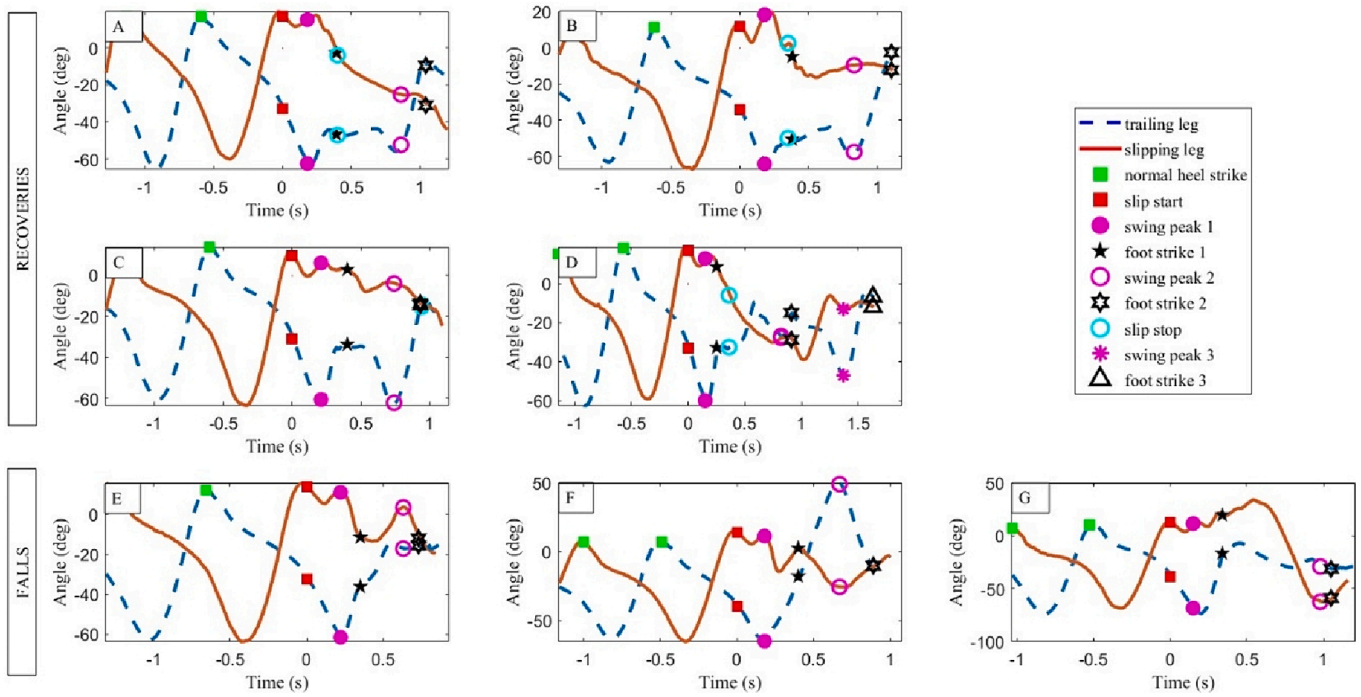

Fig. 7. Shank angle variations during one complete normal walking gait cycle before and after slip onset. Results for subjects that (A-D) recovered from slip Sub1-Sub4, respectively, and (E-G) subjects that experienced a fall Sub5-Sub7, respectively.

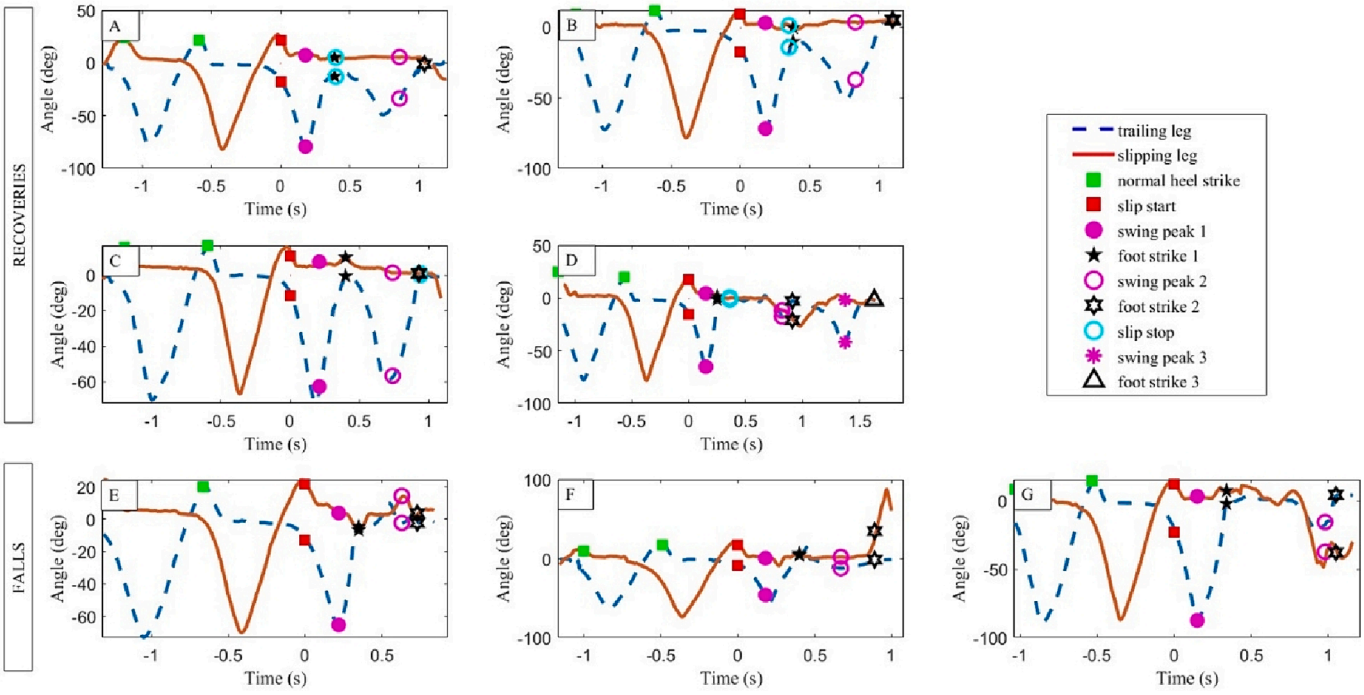

Fig. 8. Foot angle variations during one complete normal walking gait cycle before and after slip onset. Results for subjects that (A-D) recovered from slip Sub1-Sub4, respectively, and (E-G) subjects that experienced a fall Sub5-Sub7, respectively.

This study has been limited to the observations of kinematic data of the lower limbs. We have limited our analysis to the sagittal plane. Concerning the analysis of 2D data, i.e. sagittal plane joint angles, we would like to clarify that the planar covariation of "sagittal plane elevation angles" has been a topic of study in other studies. Ivanenko et al (2005) specifically suggest that planar covariation law (PCL) is violated in some conditions like stooping and Aprigliano et al. (2019) have specifically reported the violation of PCL in case of slips. This provides us with evidence that the observed effects are not due to measurement errors. Our analysis was related to the already established planar covariation law (PCL), which represents the intersegmental coordination (ISC) among the "sagittal plane limb elevation angles". Rasmussen and Hunt (2021) have reported that the largest variations of compensatory step during a slip event occur in anteroposterior direction

and that although variations exist in lateral direction, they are much smaller than those in the anteroposterior direction. Our data support similar findings for the slipping distances that were an order of magnitude grater in the A-P direction (0.31 ± 0.11 m) as compared to the medio-lateral (M−L) direction (0.03 ± 0.01 m). Therefore, the other dimensions were not considered in the current study and were out of the scope of this investigation. Future studies are required to investigate the effects caused by quantities of other dimensions and will be explored as part of our future work. The scope of slip analysis can also be expanded by including kinetic parameters like ground reaction forces, body momentum, and whole-body dynamics. Another limitation is age range of the subjects that can be expanded in future studies to generalize the results across a broader population, however, was out of the scope of this study.

In summary, we characterized the behavior of the ISC manifolds for gait after slip occurrence. Differences in the ISC manifolds were observed to deviate between fallers and recovered subject. Factors such as foot placement, foot sliding velocity, and recovery responses importantly affect the outcome of the slip leading to a fall or recovery. This initial investigation of ISC relationship during slips provides knowledge and insights about the evolution of ISC and limb angles during slip recovery. Therefore, further investigation in future studies is needed to identify generalized trends for all possible cases of recovery gaits. The knowledge and findings of the intersegmental behavior and variation of the elevation angle profiles after slip has the potential to provide insights in required responses and limb movements for successful recoveries after slip. This knowledge could be used to model the recovery process and use the models to develop effective human-inspired controllers for wearable exoskeleton devices to assist human subjects during the fall recovery process.

CRediT authorship contribution statement

Vaibhavsingh Varma: Writing – review & editing, Writing – original draft, Visualization, Investigation, Data curation. **Mitja Trkov:** Writing – review & editing, Supervision, Funding acquisition, Formal analysis, Conceptualization.

Declaration of competing interest

The authors declare that they have no known competing financial interests or personal relationships that could have appeared to influence the work reported in this paper.

Acknowledgement

This material is based upon work partially supported by the National Science Foundation under Grant No. 2301816.

References

Aprigliano, F., Monaco, V., Micera, S., 2019. External sensory-motor cues while managing unexpected slippages can violate the planar covariation law. J. Biomech. 85, 193–197.
Bianchi, L., Angelini, D., Lacquaniti, F., 1998. Individual characteristics of human walking mechanics. Pflügers Archiv 436, 343–356.
Borghese, N.A., Bianchi, L., Lacquaniti, F., 1996. Kinematic determinants of human locomotion. J. Physiol. 494.
Chang, W.R., Leclercq, S., Lockhart, T.E., Haslam, R., 2016. State of science: occupational slips, trips and falls on the same level. Ergonomics 59, 861–883.
Cheron, G., Bouillot, E., Dan, B., Bengoetxea, A., Draye, J., Lacquaniti, F., 2001. Development of a kinematic coordination pattern in toddler locomotion: Planar covariation. Exp. Brain Res. 137, 455–466. https://doi.org/10.1007/s002210000663.
Dan, B., Bouillot, E., Bengoetxea, A., Cheron, G., 2000. Effect of intrathecal baclofen on gait control in human hereditary spastic paraparesis. Neurosci. Lett. 280, 175–178. https://doi.org/10.1016/S0304-3940(00)00778-3.
Grasso, R., Zago, M., Lacquaniti, F., 2000. Interactions between posture and locomotion: Motor patterns in humans walking with bent posture versus erect posture. J. Neurophysiol. 83, 288–300. https://doi.org/10.1152/jn.2000.83.1.288. pMID: 10634872.
Hicheur, H., Terekhov, A.V., Berthoz, A., 2006. Intersegmental coordination during human locomotion: Does planar covariation of elevation angles reflect central constraints? J. Neurophysiol. 96, 1406–1419. https://doi.org/10.1152/jn.00289.2006. pMID: 16790601.
Ivanenko, Y.P., Dominici, N., Cappellini, G., Lacquaniti, F., 2005. Kinematics in newly walking toddlers does not depend upon postural stability. J. Neurophysiol. 94, 754–763. https://doi.org/10.1152/jn.00088.2005. pMID: 15728772.
Ivanenko, Y.P., d'Avella, A., Poppele, R.E., Lacquaniti, F., 2008. On the origin of planar covariation of elevation angles during human locomotion. J. Neurophysiol. 99, 1890–1898. https://doi.org/10.1152/jn.01308.2007.pMID: 18272871.
Krasovsky, T., Lamontagne, A., Feldman, A.G., Levin, M.F., 2014. Effects of walking speed on gait stability and interlimb coordination in younger and older adults. Gait Posture 39, 378–385.
Laroche, D., Ornetti, P., Thomas, E., Ballay, Y., Maillefert, J.F., Pozzo, T., 2006. Kinematic adaptation of locomotor pattern in rheumatoid arthritis patients with forefoot impairment. Exp Brain Res 176, 85–97.
Lockhart, T., Woldstad, J.C., Smith, J.L., 2002. Assessment of slip severity among different age groups. in ASTM Special Technical Publication. 1424 edn, American Society for Testing and Materials. Metrology of Pedestrian Locomotion and Slip Resistance, West Conshohcken, PA, United States, 6/5/01, pp. 17-32.
Liu, C., Finley, J.M., 2020. Asymmetric gait patterns alter the reactive control of intersegmental coordination patterns in the sagittal plane during walking. Plos one 15 (5), e0224187.
Lockhart, T.E., Smith, J.L., Woldstad, J.C., 2005. Effects of aging on the biomechanics of slips and falls. Hum Factors 47, 708–729.
Nazifi, M.M., Beschorner, K., Hur, P., 2020. Angular momentum regulation may dictate the slip severity in young adults. PLoS One 15, 1–11. https://doi.org/10.1371/journal.pone.0230019.
Noble, J.W., Prentice, S.D., 2008. Intersegmental coordination while walking up inclined surfaces: age and ramp angle effects. Exp. Brain Res. 189, 249–255.
Pai, Y.C., Bhatt, T.S., 2007. Repeated-slip training: an emerging paradigm for prevention of slip-related falls among older adults. Phys. Ther. 87, 1478–1491.
Rasmussen, C.M., Hunt, N.H., 2021. Unconstrained slip mechanics and stepping reactions depend on slip onset timing. J. Biomech. 125, 110572 https://doi.org/10.1016/j.jbiomech.2021.110572J.
Redfern, M.S., Cham, R., Gielo-Perczak, K., Grönqvist, R., Hirvonen, M., Lanshammar, H., Marpet, M., Pai IV, C.Y.C., Powers, C., 2001. Biomechanics of slips. Ergonomics 44, 1138–1166.
Schreiber, C., Moissenet, F., 2019. A multimodal dataset of human gait at different walking speeds established on injury-free adult participants. Sci. Data 6, 111.
Trkov, M., Chen, K., Yi, J., Liu, T., 2019. Inertial sensor-based slip detection in human walking. IEEE Trans. Autom. Sci. Eng. 16, 1399–1411. https://doi.org/10.1109/TASE.2018.2884723.
Winter, D.A., 2009. Chapter 4. In: Anthropometry. John Wiley & Sons Ltd., pp. 82–106. https://doi.org/10.1002/9780470549148.ch4